

EXAFS study of local atomic order about iodine in thyroxine, rat, human and sheep thyroids

 B. R. Orton^{a*} and R. Bilsborrow^b
^aDepartment of Electrical and Computational Engineering, Brunel University, Uxbridge UB8 3PH, UK, and ^bSTFC Daresbury Laboratory, Daresbury, Warrington WA4 4AD, UK.

E-mail: brianorton@waitrose.com

Radioactive ¹²⁵I emits short-range Auger electrons and represents a human health risk when incorporated in thyroglobulin of the thyroid. Quantitative evaluation of this risk can only be realised if local atomic order about iodine in the thyroid is known. Here, extended X-ray absorption fine structure (EXAFS) has been used to probe the local structure about iodine in pure thyroid hormone, thyroxine. These data are consistent with a model where iodine is bound to a single iodinated carbon ring linked to an oxygen atom, similar to a previously published model for monoiodotyrosine, a major iodinated residue in thyroglobulin. Several structural models for the local environment of iodine from rat, human and sheep have been tested and these data are found to be compatible with a slightly modified environment with respect to that found for thyroxine. The best-fit models include the following three components: (i) iodine covalently bonded to a tyrosine ring, as found for thyroxine; (ii) iodine bonded quasi-covalently to a carbonyl ligand in partially filled (50%) sites; (iii) partially filled sites (50–40%) of carbonyl ligands, with oxygen at van der Waals distances from iodine. Advantages of using Fourier-filtered EXAFS for complex crystal structures are discussed.

 © 2008 International Union of Crystallography
 Printed in Singapore – all rights reserved

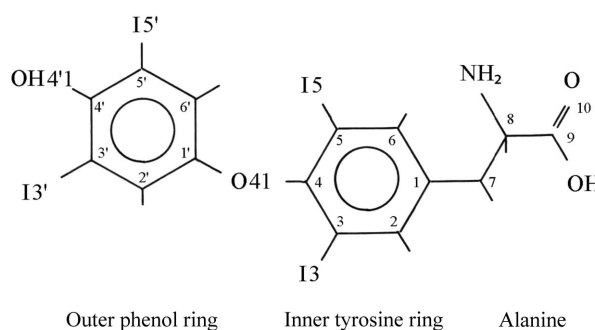
Keywords: EXAFS; thyroxine; thyroids; Auger electrons; radiation risk.

1. Introduction

In most species the thyroid is the source of the hormones thyroxine (T₄) and triiodotyrosine (T₃). These hormones have an important function in maintaining life. The biological role is determined by the structures of T₄ and T₃, together with the chemical properties of iodine. The crystal structure of T₄ (Cody, 1981) consists of an alanine residue on an inner tyrosine ring linked to an outer phenol ring by a flexible oxygen bond. Relative orientations of the almost planar rings result in I atoms forming an irregular tetrahedron with average iodine–iodine interatomic distances of 6.49 Å (Fig. 1).

T₄ with precursors monoiodotyrosine (MIT), diiodotyrosine (DIT) and triiodotyrosine (T₃) are formed and stored in thyroid follicles by a 660–670 kD dimeric polypeptide, thyroglobulin (Tg) (Dunn, 1996; Despande & Venkatesch, 1999). Iodine for hormone production is ingested from food and drink. Iodine enters the blood stream as iodate (I⁻) to be extracted at the basolateral end of a thyroidal cell, transported through the cell by Na⁺/I⁻ symporter to the lumen of follicular cells. Within the colloid of the follicle, organification of I⁻ into tyrosine residues on Tg takes place close to the apicile membrane. T₄ is formed by coupling two iodinated tyrosine residues of Tg (Taurog, 1996; Dunn *et al.*, 1998; Dunn & Dunn,

1999). When hormones are required, endocytosis of iodinated Tg takes place. T₄ and T₃ are released into the bloodstream leaving deiodinated Tg and I⁻ in the cell (Kaminsky *et al.*, 1993; Taurog, 1996; Dunn, 1996; Nilsson, 1999). Thus, iodine passes through cells twice and is stored in Tg close to the surface of thyroid cells. Should this iodine be radioactive ¹²⁵I, emissions of short-range Auger electrons close to cell nuclei could damage cell DNA. ¹²⁵I may be acquired by the thyroid


Figure 1

L-thyroxine (T₄) structure (Cody, 1981, 1996). φ , C5–C4–O41–C1' = 108.1°; φ' , C4–O41–C1'–C6' = –30.0°; χ^2 , C2–C1–C7–C8 = 162.8°; χ^1 , C1–C7–C8–N8 = –169.6°; ψ , N8–C8–C9–O9 = –40.8.

from radioactive waste in potable water (Bowl & Howe, 1992) and by users of radiopharmaceuticals. Control of radiation risk from radioactive liquid waste to watercourses is exerted by amounts of ^{125}I delivered to drainage systems. Further, adventitious biological control of amounts entering potable water takes place by absorption of ^{125}I in the aquatic environment (Vorsatz *et al.*, 1995), prior to extraction for household use. When human ingestion takes place, ^{125}I is stored in thyroidal Tg. ^{125}I has a long effective biological half-life in the thyroid (Maxon & Saenger, 1996). Auger electrons have a large, but uncertain, relative biological effect (CERRIE, 2003). In CERRIE (2003) it is stated that use of isotopes emitting Auger electrons represents a significant radiation risk. Estimates of energy deposited in thyroid follicles have been carried out by various authors (*e.g.* Ünak & Ünak, 1991). To make a better assessment an estimate must be made of emanations from Tg to thyroid cells. This can only be done if local atomic order about iodine in Tg is known (Hofer, 1996). In the same symposium that included the paper by Hofer (1996), Orton *et al.* (1996) showed that local order could be obtained using iodine L_{III} EXAFS from T_4 and Tg. This limited EXAFS study indicated that more work was required.

The new work uses I K -shell X-ray absorbance and theoretical EXAFS takes into account the polyvalent character of iodine. Cody & Murray-Rust (1984) found that iodine, in many crystal structures, sustains a covalent bond together with a weaker short quasi-covalent bond, $\text{C}-\text{I}\cdots\text{O}$. Short $\text{I}\cdots\text{O}$ distances were found from T_4 and 3,3'-diiodo-L-tyrosine to carbonyl ligands in transthyretin (Wojtczak *et al.*, 1992, 2001).

The objectives of the present work were (i) to obtain a model for T_4 EXAFS, and (ii) to apply this model to EXAFS from thyroid materials with the additions of short quasi-covalent bonds between iodine and carbonyl ligands. Materials taken directly from thyroids were used because they do not need elaborate preparation and can correspond closely to *in vivo* conditions. The disadvantages were that concentrations of iodine in these materials were small and EXAFS was weak. For this and other reasons, given below, Fourier filtering of experimental EXAFS was required.

2. Method and materials

Fine structure at an X-ray absorption edge, owing to near-neighbour interactions with photoelectrons, has been known for more than 70 years. A summary of early measurements was given by Compton & Allison (1935) and included the early theory due to Kronig. Stern (1974) gave a general theory of EXAFS that showed (Lytle *et al.*, 1975; Stern *et al.*, 1975) that it was determined by the surroundings of absorbing atoms. Also, away from the absorption edge, Fourier-transforming oscillations in EXAFS spectra gave interatomic distances and coordination numbers. An equivalent EXAFS theory by Lee & Pendry (1975) was developed by Gurman *et al.* (1984, 1986) for analysis of X-ray absorption spectra. Interpretation of the spectra using Fourier transformations of EXAFS spectra was replaced by comparison between experimental EXAFS and theoretical EXAFS derived from model structures (Binsted *et al.*, 1992; Binsted, 1998). This is the method used in the present paper.

et al., 1992; Binsted, 1998). This is the method used in the present paper.

Iodine K -shell (33.5 keV) X-ray absorbance, $\mu(E)$ (where E is the X-ray photon energy), was measured on SRS station 16.5 at Daresbury Laboratory, UK, for L- T_4 (3',5',3,5,-tetraiodo-L-tyrosine, $\text{C}_{15}\text{H}_{11}\text{I}_4\text{NO}_4$) (Sigma-Aldrich, T2376; Lot 87H1191) and the following three thyroids:

(i) Thyroids taken from six freshly killed rats. Thyroids were frozen and EXAFS was recorded 24 h after the death of the rats.

(ii) Human thyroids taken after natural death, dried, and used to measure ^{125}I content (Bowl & Howe, 1992). EXAFS measurements were made several years after the death of the carriers of the thyroids.

(iii) Thyroid extracted from a thorax of a recently killed sheep from a local abattoir. The exact history of the sheep and the thorax was not known. EXAFS examination was probably made a few days after the death of the sheep.

The history of the thyroids examined was expected to influence the agreement with any model proposed.

EXAFS from L- T_4 was obtained by transmission, but, owing to small concentrations of iodine in thyroids [0.1% to 1.1% iodine in human Tg (Taugog, 1996)], fluorescence measurements were used (Hasnain *et al.*, 1984). Repeated measurements of $\mu(E)$ at liquid- N_2 temperatures were averaged to reduce noise.

Experimental EXAFS were Fourier filtered to 5 Å using *EXCURV98* (Binsted *et al.*, 1992; Binsted, 1998) to reduce noise and restrict the complexity of theoretical models. In the analysis that follows, 'experimental EXAFS' refers to Fourier-filtered EXAFS.

The quality of least-square fit between N values of experimental and theoretical EXAFS functions, $\chi^{\text{exp}}(k)$ and $\chi^{\text{th}}(k)$, is given as a percentage by R_{EXAFS} , where

$$R_{\text{EXAFS}} = \sum_i^N (1/\sigma_i) [\chi^{\text{exp}}(k_i) - \chi^{\text{th}}(k_i)]^2 \times 100,$$

where σ_i is a normalization term, obtained from

$$(1/\sigma_i) = k_i^n / \sum_j^N k_j^n |\chi_j^{\text{exp}}(k_j)|.$$

To use a structurally plausible model, internal bond distances are restrained to defined limits (Binsted *et al.*, 1992).

Departures from restrained models are defined by R_{DISTANCE} , where

$$R_{\text{DISTANCE}} = \sum_i (1/\sigma_i) (|r_i^{\text{ref}} - r_i^{\text{ideal}}|) / r_i^{\text{ideal}} \times 100.$$

Here, r^{ref} is the refined bond distance for the model and r^{ideal} is the ideal bond distances from the crystal structure on which the model is based. R_{DISTANCE} is the percentage mean error in restrained bond lengths.

The total R -factor is defined as $R = R_{\text{EXAFS}} + R_{\text{DISTANCE}}$. It is also possible to take into account an R -factor for angles, but it was not used in the present work.

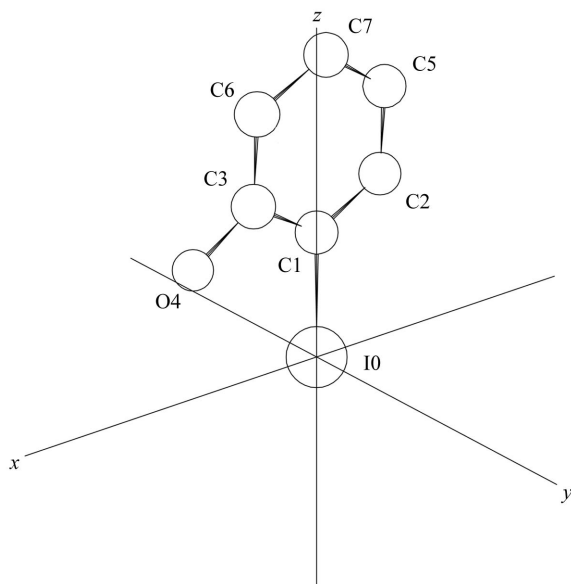


Figure 2
Theoretical model for thyroxine (T_4) EXAFS.

The preferred model had the lowest value for R in the range 15–40. However, over-determinacy of the model must be taken into account using the reduced χ^2 function (ε_v^2), given by

$$\varepsilon_v^2 = [1/(N_i - p)](N_i/N) \sum_i^N (1/\sigma_i)^2 [\chi^{\text{exp}}(k_i) - \chi^{\text{th}}(k_i)]^2,$$

where N_i is the number of independent points, p is the number of model parameters, and $N_i - p$ must always be positive. Finding the lowest value of R with the lowest ε_v is the aim of these model refinements.

All theoretical EXAFS were computed from models described below using the *EXCURV98* program. Phase changes were obtained using Hedin–Lundquist complex exchange and correlation potentials. Multiple scattering had a strong influence on calculated EXAFS owing to use of a rigid molecular model with certain atoms being almost collinear (Figs. 2 and 3). Small atom theory was used with second- and third-order scattering events included. The maximum path length was 12 Å and the minimum scattering angle was 60°. A maximum of three different atoms were in multiple-scattering paths.

3. Models and results

3.1. Thyroxine

The T_4 model was obtained from the crystal structure of T_4 *n*-dietholamine, $(C_{15}H_{10}I_4NO_4)^+ \cdot (C_4H_{12}NO_2)^-$ (Cody, 1981). This structure contained two similar arrangements of T_4 , T_{4-1} and T_{4-2} , that had almost equal interatomic distances. As mentioned above, and shown in Fig. 1, T_{4-1} consisted of an alanine residue bonded to an inner iodinated tyrosine ring with an oxygen bridge to an outer iodinated ring to give a 3,5,3',5'-iodine arrangement (Cody, 1996). Experimental EXAFS was an average from these four I atoms. I3 in T_{4-1}

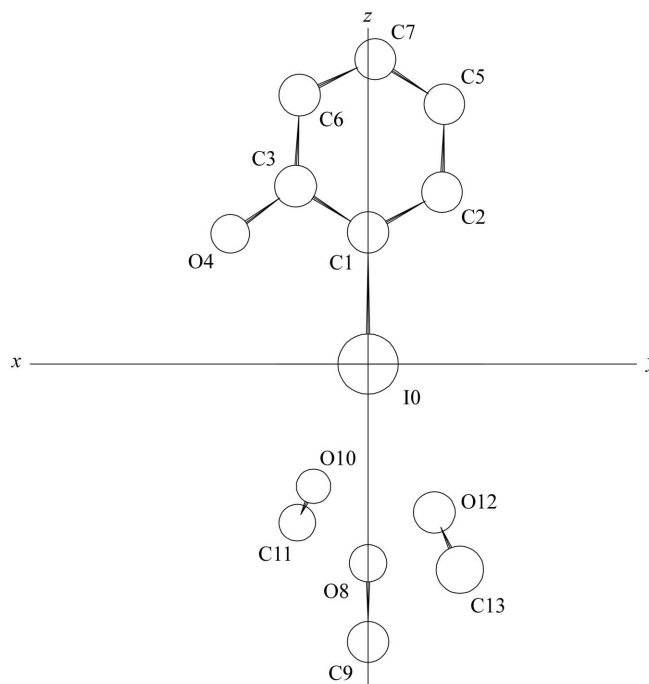


Figure 3
Theoretical model for EXAFS from rat thyroids. Carbonyl ligands (O8–C9) are indicated by site numbers given in Table 2.

provided an initial set of 23 interatomic distances for calculating theoretical EXAFS with $R_{\text{EXAFS}} = 33.8$. These 23 backscattering distances resulted in too many variables to be adjusted, compared with the number of experimental points. A simpler model was required. A similar situation existed in the model used for copper EXAFS from tetrakis(imidazolyl)copper (II) dinitrate (Binsted *et al.*, 1992) where EXAFS was matched by backscattering from a single imidazole ring. Non-Fourier-filtered EXAFS from T_4 showed weak contributions to backscattering from the remaining I atoms, so further simplifications were required. By Fourier-filtering to 5.0 Å, a distance smaller than the average iodine–iodine distance of 6.49 Å, we could eliminate all I–I interactions and greatly simplify the model. This restriction gave a model that contained 16 atoms. Non-significant atoms were removed (Binsted *et al.*, 1992) to give a final model that consisted of a central I atom with seven other atoms (Fig. 2). To reduce the number of variables further in all models, sites C2, C3 and C5, C6 were treated as equivalent pairs in terms of radial distances and Debye–Waller factors. Without this treatment their respective differences in radial distances (I0–C1 and I0–C2) were lower than the expected EXAFS resolution of 0.02 Å (Charnock, 2004).

The best fit to Fourier-filtered EXAFS using this model (Fig. 4) gave the following values: $R = 19.22$, $R_{\text{EXAFS}} = 18.48$, $\varepsilon_v^2 = 0.196 \times 10^{-6}$. Table 1 lists interatomic distances in the tyrosine ring, as well as iodine-to-atom distances used to calculate theoretical EXAFS. Tyrosine ring distances were restrained (Binsted *et al.*, 1992) to average distances from T_{4-1} (Cody, 1981) to give $R_{\text{DISTANCE}} = 0.74$ (Table 2). The reason for the success of this model can be seen from Figs. 1 and 2.

Table 1
Interatomic distances for T₄.

Fig. 2 Displays locations	T ₄ ring distances (Å)	Fig. 2 Displays locations	I0-atom distances (Å)	Debye–Waller factors, <i>a</i> (Å ²)
I0–C1	2.10	I0–C1	2.10 (2.07)†	0.003 (0.006)†
C1–C2	1.42	I0–C2	3.04 (3.02)†	0.006 (0.005)†
C1–C3	1.38	I0–C3	3.04 (3.03)†	0.006 (0.005)†
C2–C5	1.41	I0–O4	3.19 (3.14)†	0.026 (0.011)†
C3–O4	1.37	I0–C5	4.37 (4.33)†	0.014 (0.011)†
C3–C6	1.42	I0–C6	4.37 (4.37)†	0.014 (0.011)†
C5–C7	1.39	I0–C7	4.89 (4.88)†	0.016 (0.012)†
C6–C7	1.40			

† I0-atom distances and Debye–Waller factors in parenthesis are from Feiters *et al.* (2005).

The model used (Fig. 2) is similar to the arrangement of atoms about each of the four I atoms in T₄ (Fig. 1).

In Table 1 radial iodine-to-atom distances (*e.g.* I0–C1) and Debye–Waller factors are compared with those found for theoretical EXAFS from MIT (Feiters *et al.*, 2005). Within the resolution of the present work, experimental EXAFS from T₄ can be reproduced using a model similar to that used by Feiters *et al.* (2005) for MIT. The difference between the T₄

and MIT models is that an O atom at 5.22 Å, from the alanine residue, was included in the model for MIT.

3.2. Thyroids

Taurog (1996) reported that the iodine content of human thyroids varied between 0.1% and 1.1%. The fraction of inorganic iodine in thyroids was lower than 0.25% of this total. The majority of iodine was in the form of iodinated tyrosine in Tg. For human Tg that contained 0.52% iodine, the number of iodinated tyrosine residues per molecule in Tg was MIT 6.45, diiodotyrosine 2.28, T₃ 0.29 and T₄ 2.28.

Thus the highest proportion of iodinated tyrosine in Tg was MIT. For rat thyroids (Taurog, 1996) a large percentage was again MIT. The same iodinated tyrosines were assumed to be present in sheep thyroids. The models used for EXAFS for MIT and Fourier-filtered EXAFS for T₄ to 5 Å were sufficiently similar for Fig. 2 to be used as a starting model for EXAFS from all thyroids. However, Fourier-filtered rat EXAFS and theoretical EXAFS (Fig. 5) using the T₄ model (Fig. 2) gave a poor fit [*R* = 36.68 and reduced χ^2 function (ε_v^2) = 0.810, Table 3]. From this result it was clear that the local order about I0 is not as simple as that found for thyroxine, and that additional components must be added to the model.

In the thyroid, iodinated tyrosines are incorporated in the thyroglobulin molecule (Tg) (Taurog, 1996). The two main chains of Tg, as in any protein (McRee, 1999), have available carbonyl ligands to which iodine could be bonded. For thyroids we propose that the I atom (I0) at the origin in Fig. 2 was quasi-covalently bonded to a carbonyl ligand (Cody & Murray-Rust, 1984). The carbonyl ligand (O8–C9) was arranged so that C1–I0··O8 was collinear in the negative *z* direction (Fig. 3 shows the complete model). The I0–O8 bond distance was initially set to 2.96 Å (Cody & Murray-Rust, 1984). It would not be expected that all I atoms would be bonded in this way, so one carbonyl ligand (O10–C11) in the *y, z* plane was added at the van der Waals distance, initially at 3.55 Å (Cody & Murray-Rust, 1984) and spherical polar coordinates $\theta = 125.4^\circ$ and $\varphi = 270.0^\circ$. This model was used for human and sheep thyroids. The model applied to EXAFS from rat thyroids had an additional van der Waals bonded carbonyl ligand (O12–C13) in the $-y, -z$ plane with *r* = 3.55 Å, $\theta = 125.4^\circ$ and $\varphi = 90.0^\circ$. Coordinates of the van der Waals bonded carbonyl ligands were chosen so that there was no multiple scattering between ligands. In the open structure of Tg, not all I atoms would be linked to carbonyl ligands, so the degree of occupancy of these sites was adjusted to give the lowest *R*_{TOTAL} value. All I0–C distances were refined to improve the agreement between theoretical and experimental EXAFS with restraints on ring distances and carbonyl O–C distances. O–C distances were restrained to a mean value for single- and double-bond distances of 1.26 Å. Final model parameters for best agreement with experiment are listed in

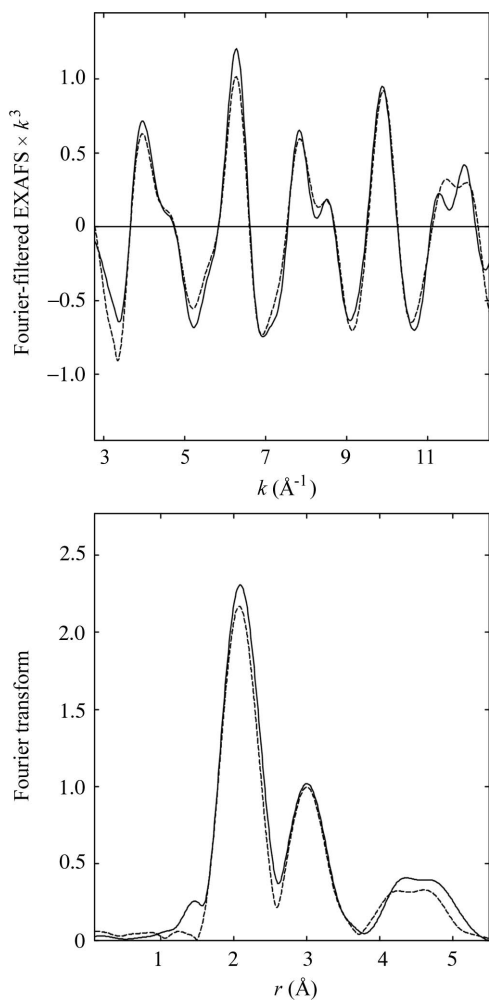


Figure 4
EXAFS from thyroxine (T₄), best theoretical fit and Fourier transform. The solid line is Fourier-filtered experimental data to 5 Å; the dashed line is theory.

Table 2

T₄ compared with thyroid materials.

E_f is the difference between the edge position and the origin of wavevector k . VPI is a constant imaginary part of the potential, accounting for losses from inelastic scattering events and related to the mean-free-path of photoelectrons (Roy & Gurman, 2001).

	T ₄		Rat		Human		Sheep	
R_{TOTAL}	19.22		27.69		33.96		37.35	
R_{EXAFS}	18.48		26.84		31.93		35.27	
R_{DISTANCE}	0.74		0.85		2.03		2.08	
$\varepsilon_v^2 \times 10^6$	0.196		0.602		0.857		4.43	
Maximum difference in C–C distances between model and average from T ₄ -1 (%)	1.97		1.79		5.44		5.69	
I-atom distances	r (Å)	a (Å ²)	r (Å)	a (Å ²)	r (Å)	a (Å ²)	r (Å)	a (Å ²)
I0–C1	2.10	0.003	2.10	0.005	2.09	0.002	2.10	0.001
I0–(C2–C3)	3.04	0.006	3.04	0.007	3.01	0.004	3.03	0.004
I0–O4	3.19	0.026	3.04	0.017	3.12	0.011	3.14	0.011
I0–(C5–C6)	4.37	0.011	4.37	0.010	4.42	0.004	4.44	0.004
I0–C7	4.89	0.016	4.83	0.010	4.93	0.005	4.95	0.005
I0–O8	Quasi-covalent bond		3.17	0.003	3.06	0.004	3.01	0.004
I0–C9			4.42	0.005	4.30	0.005	4.37	0.005
I0–O10	van der Waals bond		3.68	0.004	3.69	0.004	3.72	0.004
I0–C11			4.92	0.005	4.94	0.005	4.96	0.005
I0–O12	van der Waals bond		3.68	0.004				
I0–C13			4.92	0.005				
Site occupation			O8, C9/O10, C11/O12, C13 0.5/0.5/0.5		O8, C9/O10, C11 0.5/0.5		O8, C9/O10, C11 0.5/0.4	
E_f (eV)	−8.4 ± 0.3		−7.1 ± 0.4		−8.9 ± 0.5		−9.6 ± 0.8	
VPI	−1.2 ± 0.2		−1.6 ± 0.3		−2.4 ± 0.4		−1.6 ± 0.6	

Table 3

Theoretical T₄ model fit with thyroids.

	T ₄	Rat	Human	Sheep
R_{TOTAL}	19.22	35.68	42.41	45.62
R_{EXAFS}	18.48	34.95	41.68	44.88
R_{DISTANCE}	0.74	0.73	0.74	0.74
$\varepsilon_v^2 \times 10^6$	0.196	0.810	0.864	4.99
$\varepsilon_v^2 \times 10^6$ for complete model	0.196	0.602	0.857	4.43

Table 2 and a comparison between the experimental and theoretical EXAFS and Fourier transforms is shown in Fig. 6 for rat thyroids only.

Similar EXAFS and Fourier transforms were obtained for human and sheep thyroids, but are not displayed (they form Fig. 1 and Fig. 2, respectively, in the supplementary material¹).

4. Errors and uncertainties

There have been a number of attempts to provide a systematic method for estimates of uncertainties in EXAFS data. Methods have been compared by Newville *et al.* (1999) but only for very specific model systems under ideal experimental conditions. It is possible, however, to make some comments applicable to the procedures followed in the present work.

In §2 above, programs used to obtain experimental EXAFS are referenced. Each step carries risks of errors both random and systematic. Such errors will be reflected in the uncer-

tainties in parameters used to calculate theoretical EXAFS. Charnock (2004) suggests that uncertainties in inner-shell distances (I0–C1, Tables 1 and 2) are ±0.02 Å and for outer shells are ±0.05 Å. These errors can be classified as systematic. There are other errors treated by statistical methods contained in the *EXCURV98* program. Refinement of parameters leads to calculations of ε_v^2 , the χ^2 parameter that demonstrates the goodness of fit of theoretical to experimental EXAFS. For ε_v^2 , Charnock (2004) quotes ±15% for low values of the fit index, R . The refinement process gave the errors in parameters E_f and VPI listed in Table 2. These errors increase as the fit between theory experimental decreases. For the quasi-covalent sites, fractional occupation can only be determined to ±0.1. Fourier filtering of all experimental EXAFS to 5.0 Å reduces the number of parameters used to describe structural models and limits errors from this source.

5. Discussion of results

The complete crystal structure of T₄ (Fig. 1) contains four I atoms. It is proposed that the structure from EXAFS up to a radial distance of 5.0 Å about each I atom is given by the average arrangement shown in Fig. 2. This structure is very close to that used for theoretical EXAFS from MIT by Feiters *et al.* (2005). The largest difference between the two models is in the radial distances (Table 2) for I0–O4 (Fig. 2). This is because O4 in the T₄ model represents both the bridging oxygen between the two tyrosine rings and the hydroxyl oxygen bonded to the outer ring in T₄ (Fig. 1). In addition, the Debye–Waller factor for O4 is larger than that for C atoms at equivalent distances owing to disorder at this site. Similar

¹ Supplementary material is available from the IUCr electronic archives (Reference: GF5008). Services for accessing these data are described at the back of the journal.

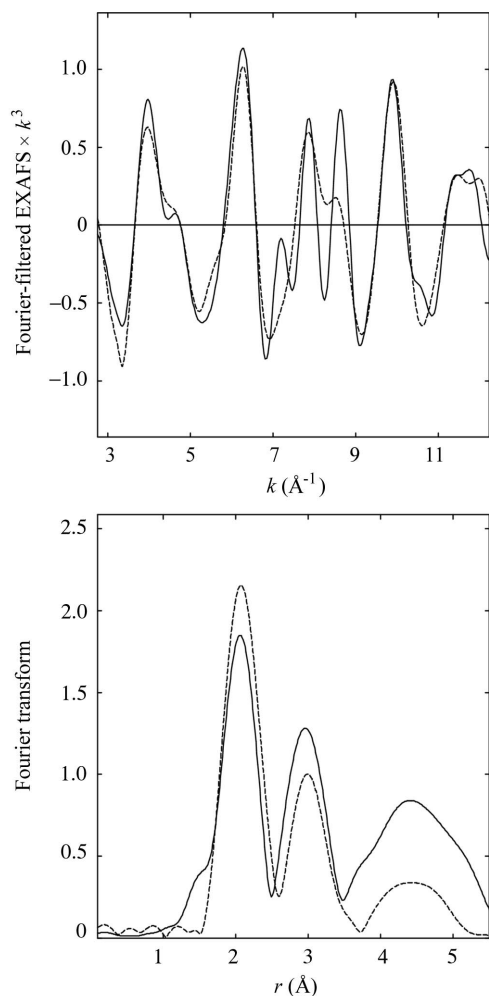


Figure 5
Rat experimental EXAFS and Fourier transform compared with theoretical EXAFS from T_4 . The solid line is Fourier-filtered experimental data to 5 Å; the dashed line is T_4 theory.

large Debye–Waller factors were found for peripheral atoms to an imidazole ring (Binsted *et al.*, 1992). Table 2 lists the maximum difference in C–C ring distances between the T_4 model and crystal structure T_4 -1 (Cody, 1981) as 1.97% which is lower than the 3.9% obtained by Binsted *et al.* (1992) for their restrained model for imidazole ring distances. Within the uncertainties mentioned above (§2), the single-ring eight-atom model (Fig. 2) reproduces the Fourier-filtered experimental EXAFS for T_4 .

For each thyroid the main component of theoretical EXAFS was the model used for T_4 . The covalent I0–C1 distances (Table 2) were all within the uncertainty for a near-neighbour distance of ± 0.02 Å (Charnock, 2004) when compared with the covalent bond distance in crystalline T_4 (Cody, 1981). Table 2 shows the maximum percentage difference between C–C ring distances for the bonded models. For rat thyroids the percentage (1.79%) was lower than for T_4 , but for the other thyroids the size of the ring increases as the fit to the model declines. The model used for T_4 (Fig. 2) alone was not capable of reproducing EXAFS from thyroid materials. Table 3 lists results of applying the T_4 model to EXAFS from

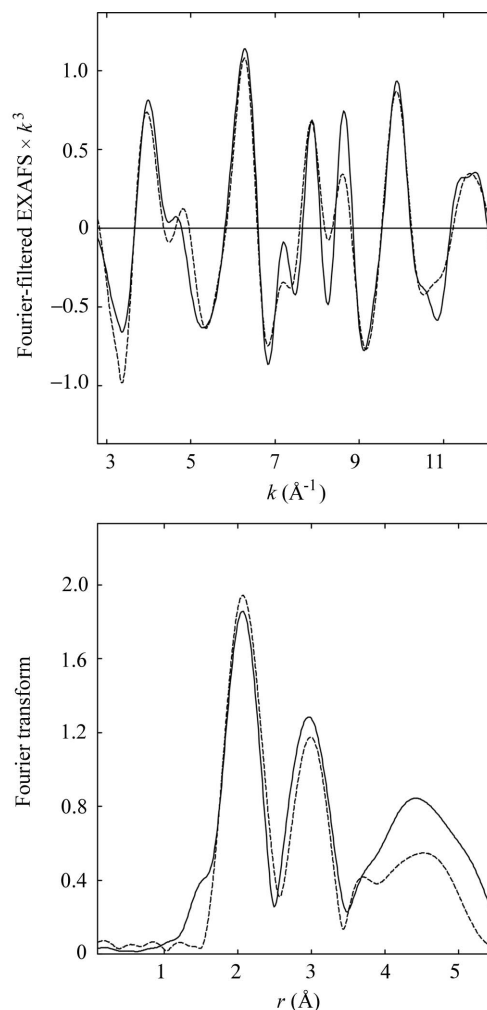


Figure 6
EXAFS from rat thyroids, best theoretical fit and Fourier transform. The solid line is Fourier-filtered experimental data to 5 Å; the dashed line is theory.

thyroids. By comparing Tables 2 and 3 it can be seen that, as more shells were added to the T_4 model, values of ϵ_v^2 and R decrease. Thus, the introduction of quasi-covalent and van der Waals bonds is essential to improve the fit (Table 2). All quasi-covalent bond distances (I0–O8) were within the range 2.66–3.52 Å proposed by Cody & Murray-Rust (1984). The average (I0–O8) was 3.08 Å, close to 3.07 Å, the distance found in T_4 bonding to rat transthyretin (Wojtczak *et al.*, 2001). However, van der Waals distances (e.g. I–O10, average = 3.69 Å) were larger than the 3.55 Å proposed by Cody & Murray-Rust (1984). The fractional occupation of quasi-covalent and van der Waals sites was equal to 0.5 for rat. For sheep thyroids the occupation of quasi-covalent bonds was 0.5 compared with 0.4 for the van der Waals bond, indicating the importance of quasi-covalent bonds. As can be seen from Table 2, iodine-to-atom distances were similar for all materials listed. Differences between model carbon–carbon and those from averaged T_4 -1 distances increased in the sequence rat, human and sheep. The fit between Fourier-filtered experimental and theoretical EXAFS declines over the sequence rat, human and sheep. However, each thyroid had a different history as

described in §2. Therefore, differences in R_{EXAFS} (Table 2) should be expected. Dissimilarity could be due to the nature of death and storage time since death of the thyroid carriers. For sheep thyroid, Tg could have become unstable, as found for human Tg (Wehner *et al.*, 2000).

We propose that quasi-covalent bonding of iodine takes place with carbonyl ligands of the secondary structure of Tg (Formisano *et al.*, 1985). Iodine from tyrosines on one of the two main Tg peptide chains could quasi-covalently bond to a carbonyl ligand from adjacent main peptide chains. This proposal is supported by an increasingly stable Tg dimer as iodine content increases (Dunn, 1996).

6. Conclusions

We have found a satisfactory model for EXAFS from T₄ to a radius of 5 Å. We have also found that quasi-covalent bonding to carbonyl ligands is present in rat, human and, to a lesser extent, sheep thyroid. Owing to the open structure of Tg, these bonds must be supplemented with van der Waals bonding to available ligands. These atoms must interact with the emission of Auger electrons from ¹²⁵I in Tg. They should be part of radiation protection calculations such as, for example, those carried out by Ünak & Ünak (1991). Further EXAFS measurements from a range of thyroid materials would be of interest in order to characterize the iodinated tyrosine interaction with Tg.

We have used EXAFS to help investigate possible detrimental effects of Auger emissions to thyroids. Auger electrons have been proposed for radiation therapy and have been investigated in depth (Hofer, 1996). To take one recent example (Vallis, 2008), ¹²⁵I has been proposed as the Auger emitting isotope to bind to androgen receptors in the treatment of prostate cancer using cancerous cells from mice. EXAFS could clarify local structure at the binding event using non-radioactive iodine in cells taken from humans. Thus risks to investigator and environment could be minimized.

BRO thanks Daresbury Laboratory for time on station 16.5 and much help from Mr J. Needham of the Daresbury Laboratory IT. Thanks are also due to Dr C. Bowl (St Bartholomew's Hospital) for providing samples of human thyroid. Help is acknowledged from Professor Gurman (University of Leicester). We also thank the referees of this paper who have made important improvements.

References

- Binsted, N. (1998). *EXCURV98, Computer program for EXAFS data analysis*, <http://srs.dl.ac.uk/XRS/Computing/Programs/excurv97/excurv98guide.htm>.
- Binsted, N., Strange, R. W. & Hasnain, S. S. (1992). *Biochemistry*, **31**, 12117–12125.
- Bowl, C. & Howe, J. R. (1992). *J. Radiat. Protect.* **12**, 59–63.
- CERRIE (2003). Committee Examining Radiation Risks of Internal Emitters. Department of Environment and Rural Affairs, London, UK.
- Charnock, J. (2004). <http://srs.dl.ac.uk/XRS/courses/Errorand%20Standards.htm>.
- Cody, V. (1981). *Acta Cryst.* **B37**, 1685–1689.
- Cody, V. (1996). *Werner and Ingbar's The Thyroid*, 7th ed., edited by L. E. Braverman and R. D. Utiger, pp. 185–189. Philadelphia: Lippincott-Raven.
- Cody, V. & Murray-Rust, P. (1984). *J. Mol. Struct.* **112**, 189–199.
- Compton, A. H. & Allison, S. K. (1935). *X-rays in Theory and Experiment*, pp. 662–671. London: Macmillan.
- Despande, V. & Venkatesch, S. G. (1999). *Biochem. Biophys. Acta*, **1430**, 157–178.
- Dunn, A. (1996). *Werner and Ingbar's The Thyroid*, 7th ed., edited by L. E. Braverman and R. D. Utiger, pp. 81–84. Philadelphia: Lippincott-Raven.
- Dunn, A. D., Corsi, C. M., Myers, H. E. & Dunn, J. T. (1998). *J. Biol. Chem.* **273**, 25223–25229.
- Dunn, J. T. (1996). *Werner and Ingbar's The Thyroid*, 7th ed., edited by L. E. Braverman and R. D. Utiger, pp. 85–95. Philadelphia: Lippincott-Raven.
- Dunn, J. T. & Dunn, A. D. (1999). *Biochemie*, **81**, 505–509.
- Feiters, M. C., Küpper, F. C. & Meyer-Klaucke, W. (2005). *J. Synchrotron Rad.* **12**, 85–93.
- Formisano, S., Moscatelli, C., Zarrilli, R., Di Jesso, B., Acquaviva, R., Obici, S., Palumbo, G. & Di Lauro, D. (1985). *Biochem. Biophys. Res. Commun.* **133**, 766–772.
- Gurman, S. J., Binsted, N. & Ross, I. (1984). *J. Phys. C*, **17**, 143–151.
- Gurman, S. J., Binsted, N. & Ross, I. (1986). *J. Phys. C*, **19**, 1845–1861.
- Hasnain, S. S., Quinn, P. D., Diakum, G. P., Wardell, E. M. & Garner, C. D. (1984). *J. Phys. E*, **17**, 40–43.
- Hofer, G. H. (1996). *Acta Oncol.* **35**, 789–796.
- Kaminsky, S. M., Levy, O., Salvador, C., Dai, G. & Carrasco, N. (1993). *Molecular Biology and Function of Carrier Proteins*, pp. 252–262. Rockefeller University Press.
- Lee, P. A. & Pendry, J. B. (1975). *Phys. Rev. B*, **11**, 2795–2811.
- Lytte, F. W., Sayers, D. E. & Stern, E. A. (1975). *Phys. Rev. B*, **11**, 4825–4835.
- McRee, D. E. (1999). *Practical Protein Crystallography*, pp. 248–256. London: Academic Press.
- Maxon, H. R. & Saenger, E. L. (1996). *Werner and Ingbar's The Thyroid*, 7th ed, edited by L. E. Braverman and R. D. Utiger, pp. 342–351. Philadelphia: Lippincott-Raven.
- Newville, M., Boyanov, B. I. & Sayers, D. E. (1999). *J. Synchrotron Rad.* **6**, 264–265.
- Nilsson, M. (1999). *Biofactors*, **10**, 277–285.
- Orton, B. R., Macovei, D. & Vorsatz, D. (1996). *Acta Oncol.* **35**, 895–899.
- Roy, M. & Gurman, S. J. (2001). *J. Synchrotron Rad.* **8**, 1095–1102.
- Stern, E. A. (1974). *Phys. Rev. B*, **10**, 3027–3037.
- Stern, E. A., Sayers, D. E. & Lytte, F. W. (1975). *Phys. Rev. B*, **11**, 4836–4846.
- Taurog, A. (1996). *Werner and Ingbar's The Thyroid*, 7th ed, edited by L. E. Braverman and R. D. Utiger, pp. 47–81. Philadelphia: Lippincott-Raven.
- Ünak, T. & Ünak, P. (1991). *Appl. Radiat. Isot.* **42**, 291–295.
- Vallis, K. A. (2008). http://science.cancerresearchuk.org/gapp/personalfund/chinafellows/oxford/oxford_projects/kavallis.
- Vorsatz, D. V., Orton, B. R., Stanton, C. M. & Adil-Smith, I. (1995). *Atoms in Our Hands*, edited by G. Marx, pp. 116–123. Budapest: Roland Eötvös Physical Society.
- Wehner, F., Wehner, H. D., Schieffer, M. C. & Subke, J. (2000). *Forensic Sci. Int.* **110**, 199–206.
- Wojtczak, A., Cody, V., Luft, J. R. & Pangborn, W. (2001). *Acta Cryst.* **D57**, 1061–1070.
- Wojtczak, A., Luft, J. & Cody, V. (1992). *J. Biol. Chem.* **267**, 353–357.